

Received: 02.02.2024

Accepted: 07.08.2024

Research Article

Discovery of new small molecules inhibitors for EphB4 receptor tyrosine kinase with a fragment-based drug design approach

Amine Ballari^{a,1}, Rachid Haloui^a, Ossama Daoui^a, Khaoula Mkhayar^a, Khadija Khaddam Allah^a, Samir Chtita^b, Abdelmoula El Abbouchi^c, Souad Elkhattabi^a

^aLaboratory of Engineering, Systems, and Applications, National School of Applied Sciences, Sidi Mohamed Ben Abdellah-Fez University, BP Box 72, Fez, Morocco

^bLaboratory of Analytical and Molecular Chemistry, Faculty of Sciences Ben M'Sik, Hassan II University of Casablanca, B.P 7955 Casablanca, Morocco

^cEuromed Research Center, Euromed Faculty of Pharmacy and School of Engineering in Biomedical and Biotechnology, Euromed University of Fes (UEMF), Meknes Road, 30000 Fez, Morocco

Abstract: Erythropoietin-producing hepatocellular carcinoma B4 (EphB4) belongs to the Eph family of receptor tyrosine kinases (RTKs) and plays a significant role in the amplification of many kinds of cancers such as lung cancer, head and neck cancer, and mesothelioma. In this work, we applied a fragment-based drug design strategy to find novel Ephb4 receptor inhibitors as potential therapeutic candidates. A screening of over 269,000 fragments from various libraries has been conducted to determine their affinity for binding EphB4. Using Schrödinger software, 1,000 fragments with the highest docking scores underwent fragment linking to generate 100 new molecules. The EphB4 binding affinity and ADMET characteristics of the top 20 docking score molecules were then examined in more detail. After the best compounds were selected, a molecular dynamics study was conducted to determine the stability of the ligand-receptor complex in the top three molecules. The resultant compound may be investigated further in the context of tyrosine kinase inhibitor drug development.

Keywords: Tyrosine kinase inhibitors, EphB4, Fragment-based drug design, Molecular docking, Molecular dynamics

1. Introduction

Recent years have witnessed the successful growth of fragment-based drug design (FBDD) as a major technique for drug discovery and development in the pharmaceutical sector. Low molecular weight molecules are chosen using the FBDD method in order to target macromolecular substrates of therapeutic significance, which are often proteins. The creation of bioactive substances, such as cancer cell inhibitors, can begin with these molecular fragments since they have the ability to attach to one or multiple locations on the target [1]. Tyrosine kinases have been linked to the pathogenesis of cancer in recent research. While their activities are well-regulated in healthy cells, mutation,

overexpression, and paracrine autocrine stimulation could lead them to acquire altered functions, which can result in cancer [2]. EphB4 is a potential pharmacological and immunotherapy target. Through September 2021, the FDA authorized 73 small molecule kinase inhibitor medications, sixteen of them targeted Ephb4 [3]. Since it has a high affinity for a variety of kinases, Staurosporine, a natural substance derived from indolocarbazole, is a typical instance of ATP-competitive kinase inhibitor [4], Staurosporine is considered in this study as a reference drug. There are two main subclasses of Eph receptors, EphA and EphB, making up the largest family of receptor tyrosine kinases (RTKs) [5]. With crucial and varied

¹ Corresponding Authors

e-mail: amine.ballari@usmba.ac.ma

Amine Ballari, Rachid Haloui, Ossama Daoui, Khaoula Mkhayar, Khadija Khaddam Allah, Samir Chtita, Abdelmoula El Abbouchi, Souad Elkhattabi

involvement in a range of biological activities during embryonic development, they constitute a key system of cell communication. Nevertheless, it has been suggested that deregulation of the Eph/ephrin interactions contributes to angiogenesis, metastasis, and tumour formation in cancer. EphB4 is implicated in head and neck cancer, lung cancer, and mesothelioma, among other upper aerodigestive malignancies. Numerous tumour types, including those of the breast, colon, bladder, endometrial, and ovary, have been linked to overexpression of EphB4. EphB4's involvement in cancer is not entirely understood. On the one hand, EphB4 expressed on tumour cells can interact with endothelial ephrinB2, promoting tumour angiogenesis and development; on the other hand, EphB4 has been documented to either promote or restrict tumour growth, depending on the tumour type and model studied. EphB4 signalling contradictions in cancer have been lately explored [6].

Fragment-based drug discovery (FBDD) is an effective method for developing efficient molecular compounds from fragments that bind weakly to the target. Because FBDD has several benefits over high-throughput screening programs, it is quickly becoming a popular technique in target-based drug development. Using this method, several powerful inhibitors of various targets have been produced. In FBDD, fragment screening methods and understanding fragment-binding mechanisms are crucial [7]. Fragment hit detection has increased due to recent advancements in computational tools and methodology for fragment-based approaches. Finding the target protein structure is usually the first step in this process, which is then followed by the creation of virtual fragment libraries, docking, and hit confirmation through the use of molecular dynamics modelling [8].

2. Computational Method

2.1. Data and software

The RCSB PDB database provided the crystal structure of the tyrosine kinase receptor EphB4. Several online fragment-screening libraries were employed to download the fragment structures. Schrödinger Maestro v 12.5 has been employed to set up the computational fragment-based drug design investigation [9].

2.2. Preparation of protein structure

Getting the tyrosine kinase 3D X-ray crystal structure (PDB ID: 3ZEW) from the RCSB protein databank [10] is the first step. Next, with the OPLS3e force field, proceed with the protein preparation wizard in Schrödinger Maestro [11]. Ensuring structural accuracy for bond ordering, hydrogen consistency, steric tensions, and charges during protein processing is the second phase. Employing the already prepared structure to generate receptor grid is the final step.

2.3. Fragment libraries

The number of fragment structures retrieved from the diversified fragment databases available online is 269,058. These fragment libraries are Life Chemicals General and Natural Product-Like, Aurora fine chemicals, Otava general and natural product-like, Enamine natural products like, ZINC and ChemBridge. After collecting the available fragments, filtration takes place using the structure filtering tool of Schrödinger Maestro in order to eliminate structures not following the rule of three. The total number of fragments produced was 145,000. They were developed under physiological pH settings using the Schrödinger suite v 12.5 LigPrep tool [12], which generated 5 conformers of each fragment. The OPLS3e force field algorithm served to minimize ligand geometry. The conformer with the lowest energy from every molecule was then chosen for molecular docking.

2.4. Preparation of EphB4 crystal structure for molecular docking

The crystal structure of EphB4 in association with Staurosporine, PDB ID 3ZEW, has a resolution of 2.50 Å. The ligand-receptor complex has been generated and enhanced in Schrödinger using the Protein Preparation Wizard. This developed complex was employed to generate receptor grid. The receptor grid was built on EphB4's active site by using the centroid of the ligand molecule as the grid box's center. The grid coordinates for X, Y, and Z were 6.89, -9.85, and 69.58, respectively.

2.5. Fragment screening

All filtered and processed fragments were docked in the standard precision (SP) mode against the active site of EphB4 using the glide module of Schrödinger v 12.5 [13]. By calculating the all-

Amine Ballari, Rachid Haloui, Ossama Daoui, Khaoula Mkhayar, Khadija Khaddam Allah, Samir Chtita, Abdelmoula El Abbouchi, Souad Elkhatabi

atom RMSD value of the re-docked ligand with the co-crystallized ligand, the docking process was verified.

2.6. Fragment linking

The top 1,000 fragments with the highest SP docking scores were chosen for fragment linking in order to create new compounds. We used the Schrodinger library design module's "combine fragments" function to apply the direct joining of the fragments that were prepositioned at various positions along the EphB4 binding site. Typically, the combine fragment tool selects the possible links that may be made between the fragments in order to unite them. The tool's default settings were chosen such that the newly generated structures may produce a maximum of 100. Before they started linking, these fragments were inspected for Van der Waals interactions. The minimum fragment centroid distance was maintained at 2 Å, the minimum bond angle variation was set to 15°, the maximum number of fragment atoms was set to 200, and the maximum atom-atom distance from distinct fragments was maintained at 1 Å for direct joining. Each fragment's links to hydrogen or halogens were chosen to be broken and then re-joined with another fragment. Then, every atom in the recently constructed molecule was reduced to a minimum. Three rounds of fragment joining were done in total. Couples of fragments were combined in the first round; in the next round, up to four fragments might be joined using the outputs from the previous round, and further on[14].

2.7. Molecular docking and visualisation of receptor-ligand interaction

The procedure of fragment-linking generated one hundred new molecules. They were initially prepared using the LigPrep tool, similar to the preceding fragments, and then they were docked into the EphB4 (3ZEW) active site using the extra precision (XP) mode of Maestro's Glide docking module. The grid coordinates utilized for the fragment screening were also employed for the docking of new molecules. The compounds were ranked using the docking scores that were obtained. Through the use of PyMOL, the ligand-receptor interactions inside the protein's active regions were visualized. The prime tool was utilized after docking the ligand-receptor complexes to compute

the free binding energy (G_{bind}) using the Molecular Mechanics' Generalized Born Surface Area (MM-GBSA) technique. The same docking approach and MM-GBSA-free binding energy calculation were carried out for the standard drug Staurosporine target EphB4, which has been authorized for the treatment of EphB4 positive cancers, and for the tyrosine kinase EphB4 inhibitors.

2.9. Prediction of the in-silico physicochemical and pharmacokinetic properties

By applying Maestro's QikProp module[15], we investigated the virtual physicochemical properties of the novel compounds that were predicted to have strong binding affinities towards EphB4. We exploited the pkCSM machine-learning platform to predict the pharmacokinetic properties of small compounds in terms of pharmacokinetic parameters.

2.10. Molecular dynamic simulations

Using Schrödinger software, the best three compounds and Staurosporine as ligand reference in complex with 3ZEW were studied via molecular dynamic (MD) simulation for duration of 100 ns. The ligand-receptor structure generated during the molecular docking study was used to launch the simulation, and the stability of the complex was evaluated using an all-atom force field. The ligand-receptor system was built and solved by the system builder. The charged protein-containing solvate system was neutralized using Na^+ or Cl^- ions. By using the steepest descent method, the energy of the complex was reduced. It was then followed by two consecutive 100 ns long equilibration simulation phases using isobaric isothermic (NPT) and canonical (NVT) ensembles. Using the particle mesh Ewald technique, the NPT group used for the production MD simulation and long-range electrostatic interactions was found[16]. Using the Schrödinger simulation program, MD calculations were performed at 300 K temperature and 1 bar pressure. The data obtained was analysed by graphing the solvent accessible surface area (SASA), RMSD, and RMSF.

3. Results and discussion

The recent study is an application of fragment-based drug discovery to create a new molecule

Amine Ballari, Rachid Haloui, Ossama Daoui, Khaoula Mkhayar, Khadija Khaddam Allah, Samir Chtita, Abdelmoula El Abbouchi, Souad Elkhattabi

inhibitor of Ephb4 receptor tyrosine kinase from the available fragment libraries. Figure 1 shows the various components of the workflow.

3.1. Fragment database screening and linking

Various fragments totalling 269,058 have been downloaded from the online sources indicated earlier. Firstly, these fragments have been filtered applying the rule of three filters [17]. The Ro3 parameters were as follows: molecular weight: ≤ 250 , number of Hydrogen bond acceptors (HBA): ≤ 3 , number of Hydrogen bond donors (HBD): ≤ 3 , clogP: ≤ 3 , number of rotatable bonds (NRB): and ≤ 3 , and total polarizable surface area (TPSA): $\leq 60\text{\AA}$. Following the application of Ro3 filter, 145,000 fragments were retrieved. Next, the

LigPrep tool was employed to prepare all of the filtered fragments for energy minimization. Using OPLS3e force field, five low-energy conformers have been produced at physiological pH for each ligand. The molecular docking of the filtered and prepared fragments was carried out using the standard precision (SP) mode of Glide. All of the docked fragments exhibited SP docking values between -8.486 and 1.709 kcal/mol. Using Schrödinger's combine fragment tool, the top 1000 fragments with docking scores less than -6.5 have been chosen for joining in order to create 100 new compounds. The Ligprep tool is employed to prepare the newly acquired compounds while maintaining all the same settings as were used for getting the fragments previously.

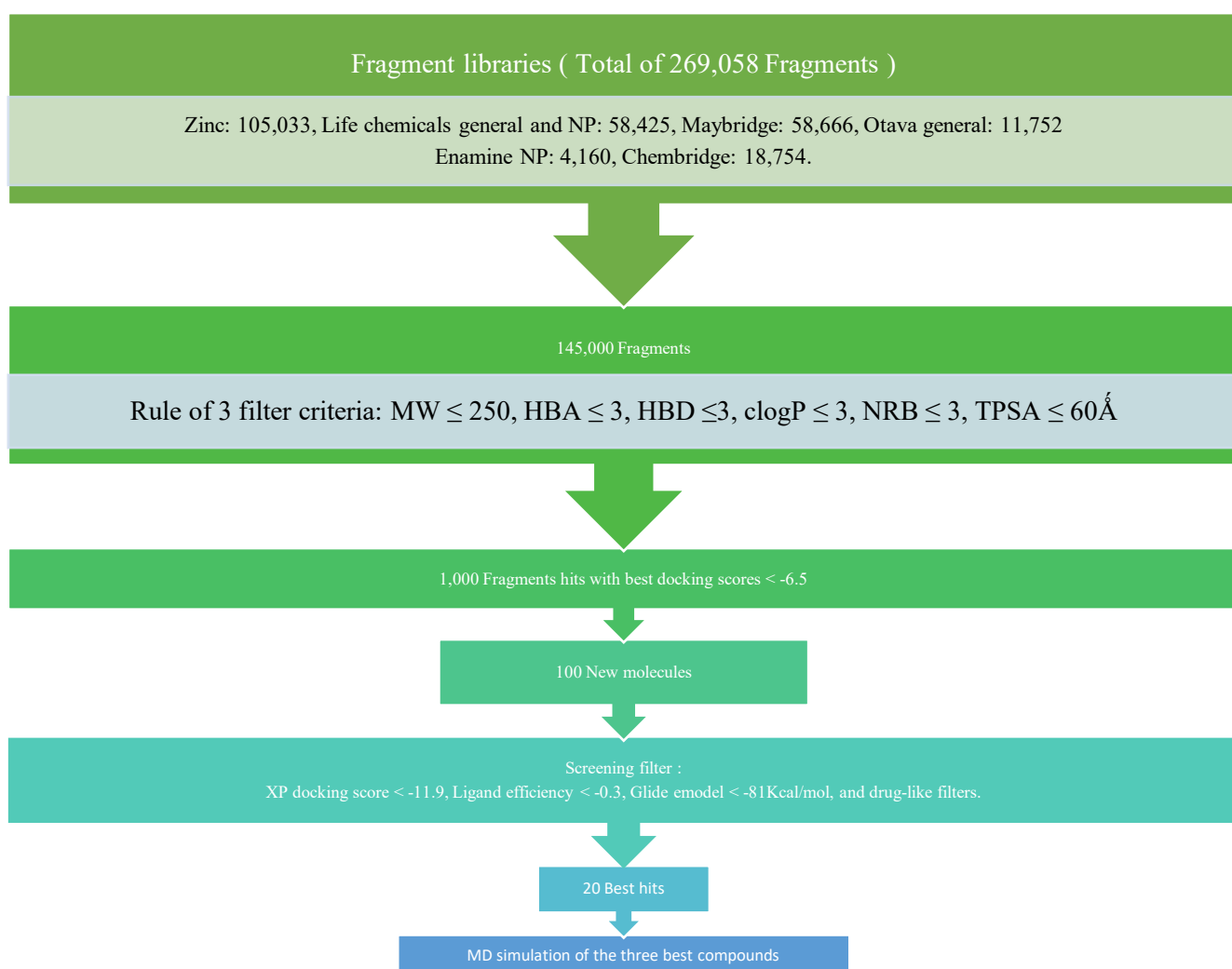


Figure 1. Schematic diagram of the FBDD workflow

Amine Ballari, Rachid Haloui, Ossama Daoui, Khaoula Mkhayar, Khadija Khaddam Allah, Samir Chtita, Abdelmoula El Abbouchi, Souad Elkhattabi

3.2. Molecular docking of newly designed compounds

By applying Glide's extra precision (XP) mode, newly developed compounds were docked to the binding site using identical grid coordinates. The twenty highest scoring compounds are presented in Table 1, with docking scores ranging from -11.934 to -14.009 kcal/mol; additionally, these compounds were evaluated based on ligand efficiency and glide energy. The estimated binding energy of a ligand to its receptor per atom is known as ligand efficiency. It may be defined as the ratio of Gibb's free energy to the number of atoms of hydrogen in the substance. It corresponds exactly with the docking score. The highest-scoring compounds had ligand efficiencies ranging from -0.486 to -0.377, indicating a high affinity for the receptor. Glide uses energy to discover the best ligand pose. The Glide Score is then used to compare these best poses. The Glide energy values of the 20 compounds in the short list range from -73.550 to -55.241 kcal/mol. The newly designed 20 compounds demonstrated important interactions with the receptor's active site. The 2D and 3D ligand-receptor interaction diagrams of the top three compounds (14, 17, and 18) are shown in Figures 3 and 4. These compounds were all created by applying Schrödinger's method to join fragments. A selection of the 1000 best-docked fragments has been made. These fragments docking scores served to rank them from 1 to 1000. Compound (14) was formed by combining rank 80 (docking score - 7.5 kcal/ mol) and rank 161 (docking score-7.23 kcal/mol) fragments by ethyl

linkage. The aromatic ring of compound (14) formed π - π stacking with Lys647, the key amino acid residue of the active site of EphB4. The compound (14) ketone groups exhibited an H-bonding with Met696 and Ala700 amino acid residues, the N-terminal showed an H-bonding with Asp45 amino acid. These amino acids are the active site residues of EphB4. Compound (17) was obtained by the linking of rank 846 (docking score - 6.578 kcal/mol) and rank 984 (docking score - 6.51 kcal/mol) fragments by a simple covalent bond linkage. The ketone group of the compound (17) showed hydrogen bonding with Glu625 and Lys647 residues of EphB4. The nitrogen of the primary amine group formed a hydrogen bond with Glu664 and Asp758 of EphB4, and both NH and N⁺H₃ created H-Bonds with Asp758 residue. Compound (18) was designed by the ethyl chain linking of rank 88 (docking score - 7.456 kcal/mol) and ranks 447 (docking score-6.849 kcal/mol) fragments. In compound (18), the ammonia radical group N⁺H₃ formed hydrogen bonding with Asp740 and Asp758 residues of EphB4. The N⁺H₂ group showed hydrogen bonding with Asp758. The nitrogen of the amine group present in the second fragment portion of the compound (18) presented hydrogen bonding with Glu664 of EphB4, this additional Hydrogen bonding provided more stability to the ligand-receptor complex. Similar forms of interactions between the other compounds and the protein's active site residues were also observed especially hydrogen bonds with Asp740, Asn745, Asp758, and Met696 amino acids.

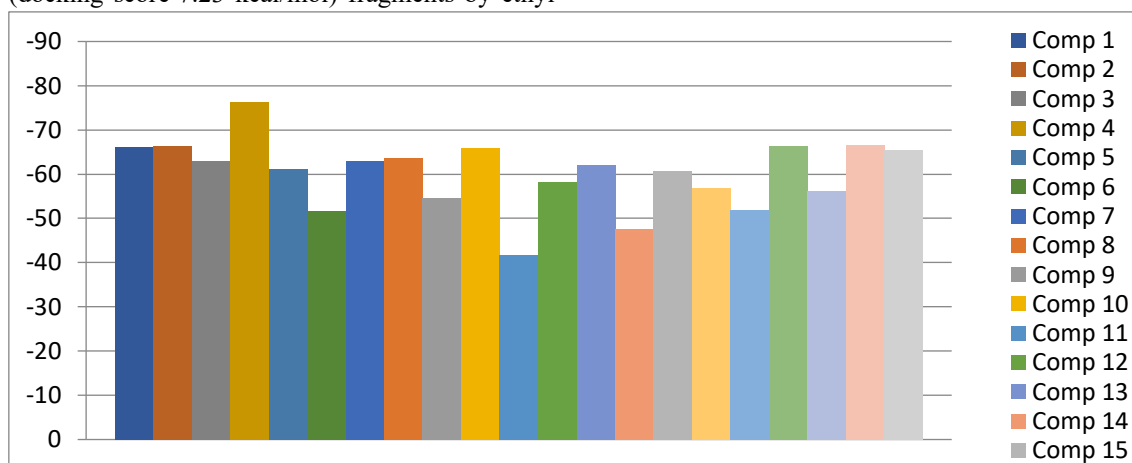


Figure 2. Compounds 1-20 and Staurosporine's MM-GBSA free binding energy values.

Amine Ballari, Rachid Haloui, Ossama Daoui, Khaoula Mkhayar, Khadija Khaddam Allah, Samir Chtita, Abdelmoula El Abbouchi, Souad Elkhattabi

3.3. MM-GBSA-free binding energy computations

Compared with all other molecular docking score parameters, the binding energy has been proven to be a more accurate screening parameter. As a way to estimate the free binding energy of ligand-receptor complexes [18], additional analysis of the docked ligand-receptor complexes was conducted by adopting the Molecular Mechanism-Generalized Born Surface Area (MM-GBSA) method. Using the software, the total free binding energy (MM-GBSA ΔG_{Bind}) was computed as follows: MM-GBSA

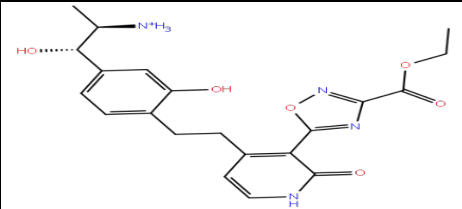
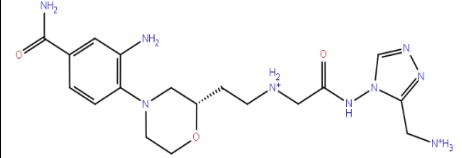
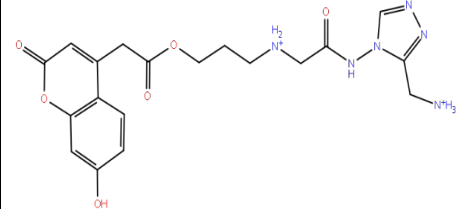
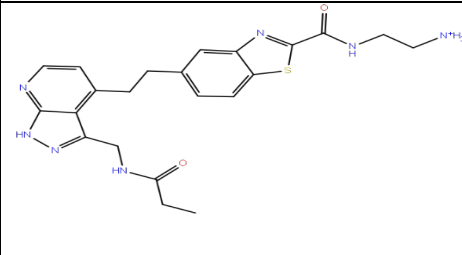
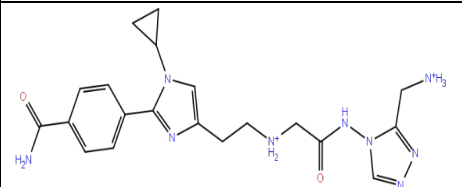
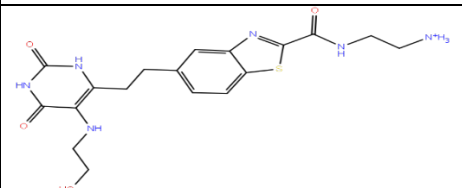
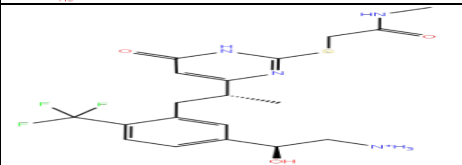
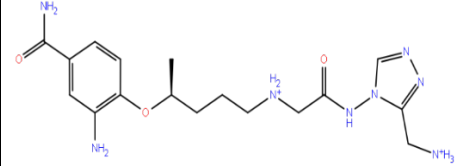
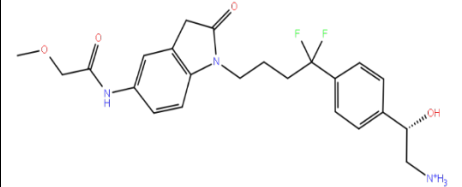
$\Delta G_{\text{Bind}} = G_{\text{Complex}} - (G_{\text{Receptor}} + G_{\text{Ligand}})$ where the energies of the optimized ligand-receptor complex are expressed by G_{Complex} , and the energies of the optimized receptor and ligand are symbolized by G_{Receptor} and G_{Ligand} , respectively.

Prime MM-GBSA employs the VSGB solvation model. Figure 2 shows MM-GBSA ΔG_{Bind} values of the top 20 compounds as well as Staurosporine as a standard EphB4 inhibitor. Compound (4) exhibits the most negative binding free energy (-76.39kcal/mol), predicted by the MM-GBSA method, and the best binding affinity for EphB4.

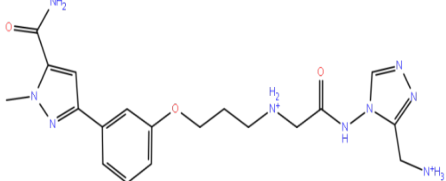
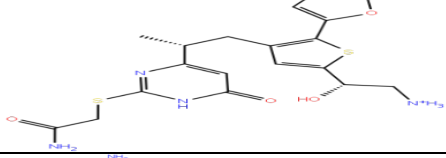
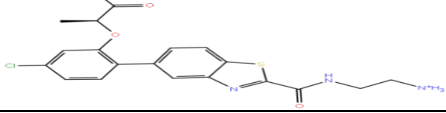
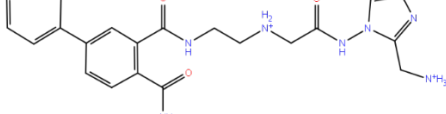
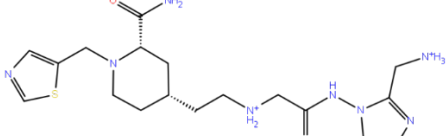
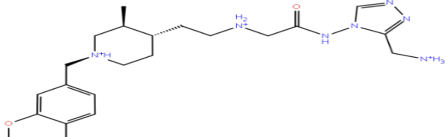
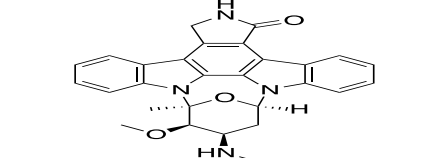
Table 1. Docking results and chemical structures of the newly generated compounds

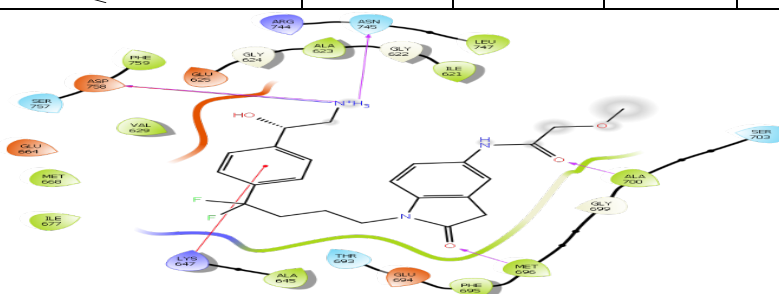
Compound Number	Structure	Docking Score (Kcal/mol)	Glide energy (Kcal/mol)	Ligand Efficiency	Residue interactions (H-bond, π - π stacking)
1		-14.009	-73.550	-0.438	Asn745, Asp758 Asp740, Met696
2		-13.950	-68.004	-0.436	Asn745, Asp758 Ala623, Ile621 Ala700, Met696 Lys647
3		-13.527	-65.528	-0.436	Asp740, Asp758 Asn745, Glu667 Met696
4		-13.490	-66.726	-0.450	Asp745 Asn758 Met696
5		-13.114	-63.813	-0.486	Asn745 Asp740 Asp758 Met696

Amine Ballari, Rachid Haloui, Ossama Daoui, Khaoula Mkhayar, Khadija Khaddam Allah, Samir Chtita, Abdelmoula El Abbouchi, Souad Elkhattabi

6		-13.051	-63.260	-0.421	Asn745, Arg744 Asp758, Met696
7		-12.991	-66.958	-0.433	Asp740, Asp758 Lys647, Thr693 Met696
8		-12.579	-68.371	-0.406	Asp740, Asp758 Glu625, Lys647 Ala700, Glu694 Met696
9		-12.428	-64.769	-0.388	Asp740 Asp758 Lys647 Glu625 Met696 Ile621 Ala700
10		-12.390	-67.775	-0.400	Asp740 Asp758 Met696
11		-12.390	-55.241	-0.427	Asp740, Asp758 Met696, Lys647 Glu625, Thr693
12		-12.375	-61.533	-0.413	Asp758, Asn745 Glu697, Met696
13		-12.373	-67.470	-0.442	Asp740, Asp758 Asn745, Thr693 Met696
14		-12.245	-58.668	-0.383	Asp758, Asn745 Ala700, Met696 Lys647

Amine Ballari, Rachid Haloui, Ossama Daoui, Khaoula Mkhayar, Khadija Khaddam Allah, Samir Chtita, Abdelmoula El Abbouchi, Souad Elkhattabi

15		-12.138	-70.529	-0.392	Asp758 Asn745 Met696
16		-12.103	-60.682	-0.417	Asp758 Met696 Glu697
17		-12.088	-61.813	-0.417	Asp758, Asp740 Lys647, Glu625 Glu664
18		-12.070	-69.616	-0.377	Asp758 Asp740 Glu664
19		-12.031	-59.332	-0.415	Asp758 Asn745 Met696
20		-11.934	-67.975	-0.385	Asp758, Asp740 Asn745, Glu625 Met696
Reference molecule Staurosporine		-5.691	-36.912	-0.163	Lys647 Ile621



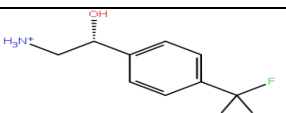
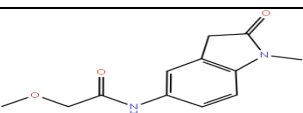
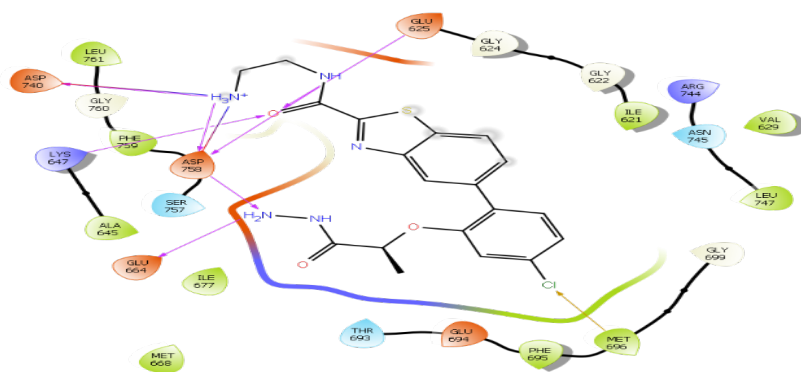
Compound 14	
Constituent fragment 1	Constituent fragment 2
Docking score: -7.5	Docking score: -7.23
Rank: 80	Rank: 161
	

Figure 3A. Ligand-receptor interaction diagram of the compound 14 at the active site of EphB4 protein (PDB ID: 3ZEW), the two constituent fragments are shown on down side.

Amine Ballari, Rachid Haloui, Ossama Daoui, Khaoula Mkhayar, Khadija Khaddam Allah, Samir Chtita, Abdelmoula El Abbouchi, Souad Elkhattabi



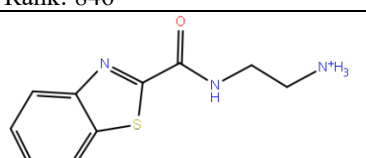
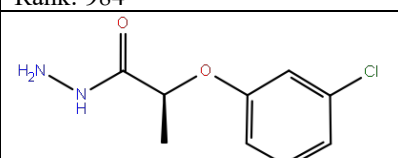
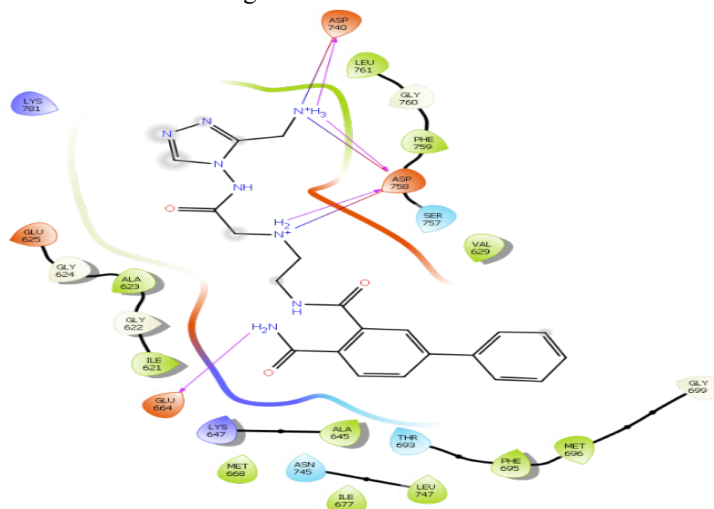
Compound 17	
Constituent fragment 1	Constituent fragment 2
Docking score: -6.578	Docking score: -6.51
Rank: 846	Rank: 984
	

Figure 3B. Ligand-receptor interaction diagram of the compound 17 at the active site of EphB4 protein (PDB ID: 3ZEW), the two constituent fragments are shown on down side.



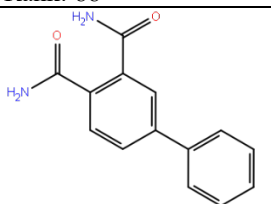
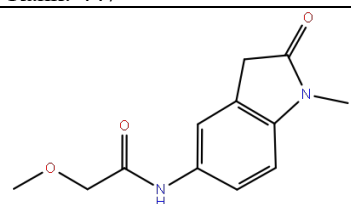
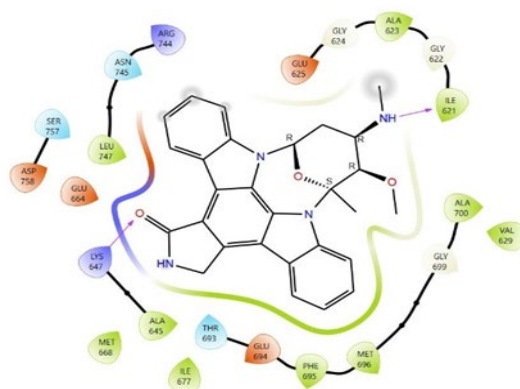
Compound 18	
Constituent fragment 1	Constituent fragment 1
Docking score: -7.456	Docking score: -6.849
Rank: 88	Rank: 447
	

Figure 3C. Ligand-receptor interaction diagram of the compound 18 at the active site of EphB4 protein (PDB ID: 3ZEW), the two constituent fragments are shown on down side

Amine Ballari, Rachid Haloui, Ossama Daoui, Khaoula Mkhayar, Khadija Khaddam Allah, Samir Chtita, Abdelmoula El Abbouchi, Souad Elkhattabi



Reference molecule: Staurosporine

Figure 3D. Ligand-receptor interaction diagram of the Staurosporine at the active site of EphB4 protein (PDB ID: 3ZEW), the two constituent fragments are shown on down side.

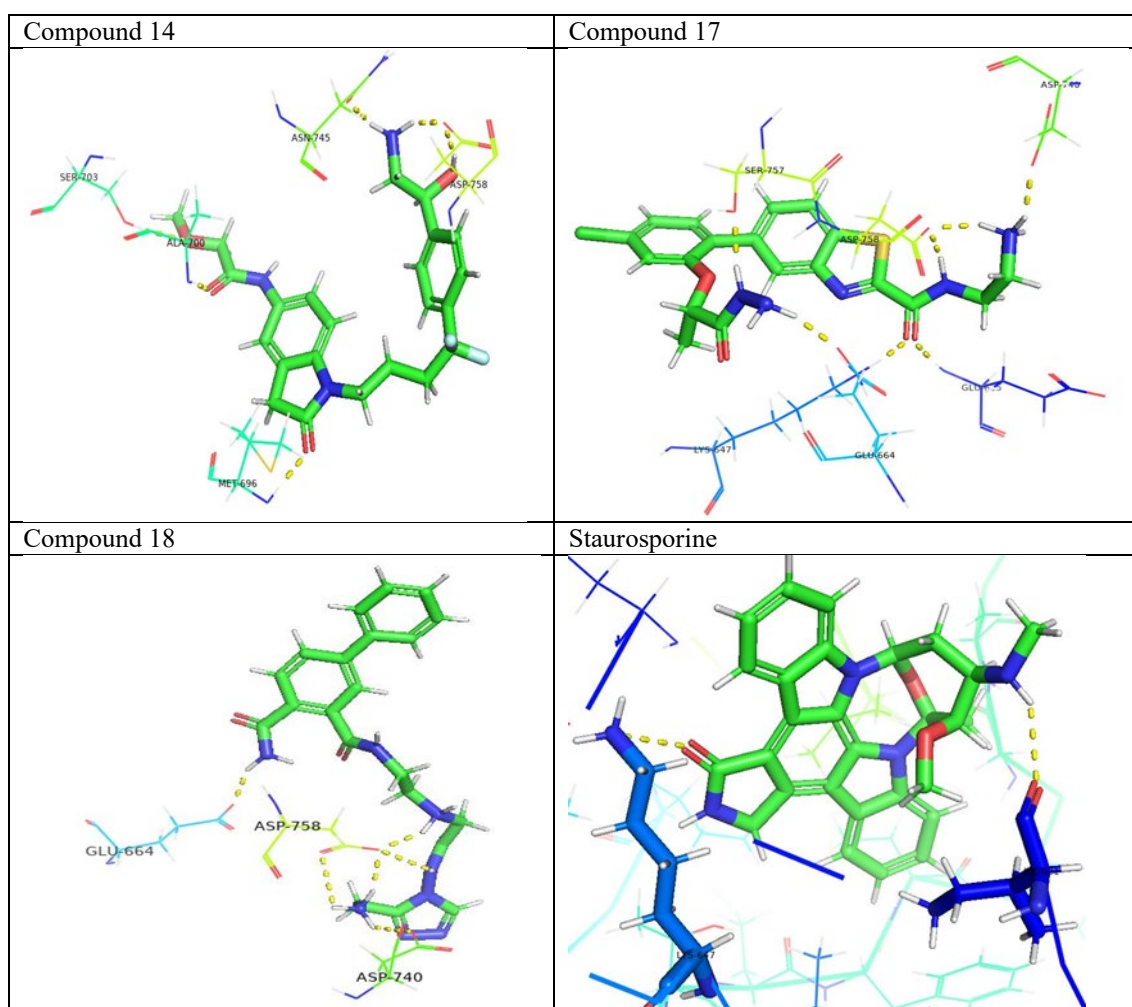


Figure 4. Ligand-receptor interactions 3D visualisation of compounds (14, 17, 18, and Staurosporine) and EphB4 with PyMol.

The binding free energies of compounds (14), (17), and (18) were -47.52, -51.89, and -66.33 kcal/mol, respectively, showing higher levels of interaction with the receptor. Although Staurosporine's binding

affinity was lower (40 kcal/mol) than that of the experimental compounds, its binding free energy was still comparable at -65.43 kcal/mol.

Amine Ballari, Rachid Haloui, Ossama Daoui, Khaoula Mkhayar, Khadija Khaddam Allah, Samir Chtita, Abdelmoula El Abbouchi, Souad Elkhatabi

3.4. Prediction of the in-silico physicochemical and pharmacokinetic properties

First, the newly generated 20 compounds were selected according to their ligand efficiency and docking scores. The resulting molecules were then evaluated for physicochemical and pharmacokinetic properties using the QikProp tool (Tables 2) and the pkCSM server (Table 3) in order to verify their drug-likeness. The optimal drug-like molecules should have molecular weight \leq 500, LogP \leq 5, number of hydrogen bond donors \leq 5, and number of hydrogen bond acceptors \leq 10, according to Lipinski's rule of five [19]. Veber and co-workers included as well two more parameters: the number of rotatable links and the topological polar surface area (TPSA) [20]. All the compounds, listed in Table 2, respect the two stated rules, with just a few exceptions.

As indicated in Table 3, the pkCSM server predicted the ADMET parameters of the twenty compounds, such as Water solubility, Intestinal absorption (human), VD_{ss} (human), BBB permeability, CNS permeability, Metabolism, Excretion, and Toxicity. In water at 25°C, a compound's water solubility indicates how soluble the molecule is. Drugs that are lipid-soluble absorb less readily than those that are water-soluble, particularly when administered internally. A substance is considered poorly absorbed if its percentage is less than 30%. Intestinal absorption is

a prediction of the percentage of compounds that diffuse through the human small intestine.

The theoretical volume required for a drug's whole dosage to be evenly dispersed in order to produce a concentration equal to that of blood plasma is known as the steady-state volume of distribution, or VD_{ss}. More of a drug is dispersed in tissue as opposed to plasma at higher VD levels. Log VD_{ss} is considered low if it is below -0.15 and high if it is above 0.4. BBB permeability evaluates a drug's capacity to penetrate into the brain; blood-brain barrier permeability is a vital factor to consider when minimizing side effects and toxicities. A molecule with a logBB value greater than 0.3 is considered to easily penetrate the blood-brain barrier, whereas molecules with a logBB value less than -1 are thought to be poorly dispersed to the brain. CNS permeability, also known as blood-brain permeability-surface area product (logPS), is measured during in-vivo brain perfusions with a substance administered directly into the carotid artery. Compounds with logPS $>$ -2 seem to be able to enter the central nervous system (CNS), whereas those with logPS $<$ -3 are thought to be unable to reach the CNS. Compounds (14), (17), and (18) were chosen for molecular dynamics based on the previously described pharmacokinetics parameters, since they had the best physicochemical and pharmacokinetics properties. Lastly, The SwissADME server was the tool used to calculate the synthetic accessibility score for the top three compounds. The results, represented in Table 4, suggest that all of the compounds are easily synthesizable.

Table 2. Predicted physicochemical parameters of compounds (1-20) and Staurosporine.

Compound number	MW (g/mol)	HBD	HBA	QLogP _{o/w}	PSA	Rotor
1	439.476	6	14.5	-1.663	200.493	11
2	464.535	6	11.9	-0.352	173.120	14
3	425.489	5	11.2	0.222	151.690	13
4	417.510	5	12	-0.586	148.571	11
5	399.839	6	13.7	-1.950	189.590	13
6	428.444	5	10.95	0.207	175.799	10
7	417.470	7	14.7	-2.431	200.062	10
8	430.419	5	13.75	-1.540	206.134	12
9	451.545	5	9.5	1.040	157.132	10
10	423.477	6	12.5	-0.770	177.659	9
11	418.470	7	11.2	-0.922	193.941	11
12	444.471	5	8.7	1.119	138.097	10
13	390.444	7.5	12.75	-1.986	197.660	13
14	447.481	4	9.9	1.841	126.720	12
15	427.465	6	12.75	-0.953	188.163	11
16	434.527	6	9.2	0.054	159.241	10
17	433.912	6	8.75	1.252	150.403	9
18	436.472	7	13.5	-1.173	194.992	11
19	421.519	6	14.5	-2.860	178.917	11
20	431.537	5	12	-0.182	147.585	12

Amine Ballari, Rachid Haloui, Ossama Daoui, Khaoula Mkhayar, Khadija Khaddam Allah, Samir Chtita, Abdelmoula El Abbouchi, Souad Elkhattabi

Staurosporine	466.541	2	4	3.09	69.4	2
Range as per QikProp module of Schrödinger	130-725	0-6	2-20	-2 to 6.5	7-200	0-15

Table 3. Predicted pharmacokinetic parameters of compounds (1–20) and Staurosporine

Compounds	Absorption		Distribution			Metabolism							Excretion	Toxicity
	Water solubility	Intestinal absorption (human)	VDss (human)	BBB permeability	CNS permeability	2D6	3A4	1A2	2C19	2C9	2D6	3A4	Total clearance	AMES toxicity
Unity	(Log mol/l)	Numeric (% absorbed)	Numeric (LogL/Kg)	Numeric (logBB)	Numeric (LogPS)	Substrate		Inhibition					Numeric (Log ml/min/kg)	Categorical (yes/no)
1	-2.906	30.275	1.341	-0.977	-4.31	No	No	No	No	No	No	No	1.219	No
2	-2.739	56.765	-0.412	-1.275	-4.387	No	Yes	No	No	No	No	No	0.997	No
3	-2.464	50.088	1.164	-0.983	-4.057	No	Yes	No	No	No	No	No	1.311	No
4	-2.481	38.489	1.084	-0.396	-4.344	No	No	No	No	No	No	No	1.288	No
5	-2.471	31.151	0.203	-1.278	-4.034	No	No	No	No	No	No	No	1.372	No
6	-2.672	53.778	0.89	-1.369	-4.162	No	Yes	No	No	No	No	No	0.82	No
7	-2.062	36.428	0.601	-0.698	-0.698	No	No	No	No	No	No	No	1.377	No
8	-2.173	43.555	0.287	-1.082	-4.33	No	Yes	No	No	No	No	No	1.312	No
9	-3.09	66.531	1.532	-1.64	-3.62	No	Yes	No	No	No	No	No	1.79	No
10	-2.894	54.02	-0.226	-0.704	-3.468	No	No	No	No	No	No	Yes	1.442	Yes
11	-2.682	45.728	0.691	-1.309	-3.995	No	No	No	No	No	No	No	1.425	No
12	-2.968	59.284	0.613	-1.059	-3.316	No	Yes	No	No	No	No	No	0.717	No
13	-2.161	35.13	0.589	-0.829	-3.472	No	No	No	No	No	No	No	1.373	No
14	-3.095	75.275	0.789	-0.844	-3.152	No	Yes	No	No	No	No	Yes	1.259	No
15	-2.678	43.915	0.57	-1.05	-3.495	No	No	No	No	No	No	Yes	0.996	No
16	-2.64	66.768	0.601	-1.216	-3.455	No	Yes	No	No	No	No	Yes	1.088	No
17	-3.399	64.663	0.354	0.354	-3.278	No	Yes	No	No	No	No	No	0.973	No
18	-2.515	41.7	1.134	-0.599	-4.415	No	Yes	No	No	No	No	No	1.124	No
19	-2.448	42.402	0.27	-0.862	-3.58	No	No	No	No	No	No	No	1.349	No
20	-2.576	39.272	1.062	-0.411	-4.334	No	No	No	No	No	No	No	1.351	No
Staurosporine	-2.788	95.188	0.185	-0.212	-3.468	No	Yes	No	No	No	No	No	-0.087	No

MW molecular weight, HBD hydrogen-bond donor atoms, HBA hydrogen-bond acceptor atoms, QPlogPo/w predicted octanol/water partition coefficient, PSA polar surface area, Rotor number of rotatable bonds,

Table 4. Synthetic accessibility scores of the three best compounds

Compounds	Synthetic accessibility scores
14	3.67
17	3.77
18	3.64

3.5. Molecular dynamics (MD)

The molecular dynamic simulations were evaluated based on the values of root mean square deviation (RMSD), root mean square fluctuation (RMSF), and radius of gyration as a function of time. The structural variation was calculated using RMSD values of protein-ligand complexes ranging from 0 to 100 ns. The average difference between the corresponding atoms of two proteins is indicated by the RMSD value (Figure.5A); the lower the RMSD, the more similar the two structures are. Throughout the simulation, compound 14's RMSD values climbed gradually from 0 to 30 ns and achieved a steady situation. Compound 17's RMSD readings revealed numerous fluctuations without any stable state. Compound 18 is the only one that displayed fluctuations similar to the protein variations and

had the smallest and most steady RMSD value all over the range of 1 to 1.5. The entire simulation's fluctuation for each atom appears in the RMSF plot (Figure. 5B). For the 270 amino acids protein Ephb4, the reference molecule, and the three possible therapeutic candidates, RMSF was computed; the results indicated that the binding site residues fluctuated slightly. Compounds 14, 17, 18, and Staurosporine had average RMSF values of 1.39, 0.92, 0.93, and 0.91 respectively. These results indicated from one side that compounds 17 and 18 have the closest average RMSF values compared to the protein average of 0.84, from another side, based on RMSF plots, the fluctuations of major peaks were observed with the backbone residue positions between Arg633-Ala645 (RMSF, 3.337 Å), Ile646-Ala665 (RMSF, 4.405Å), Ser762-

Amine Ballari, Rachid Haloui, Ossama Daoui, Khaoula Mkhayar, Khadija Khaddam Allah, Samir Chtita, Abdelmoula El Abbouchi, Souad Elkhattabi

Ptr (RMSF, 4.295 Å), and Thr775-Trp786 (RMSF, 2.802 Å) of the reference ligand in complex with EphB4. Compared to the three compounds, the complex protein-ligand 18 showed similar

fluctuations as the reference compounds. This confirms the stability of compound 18.

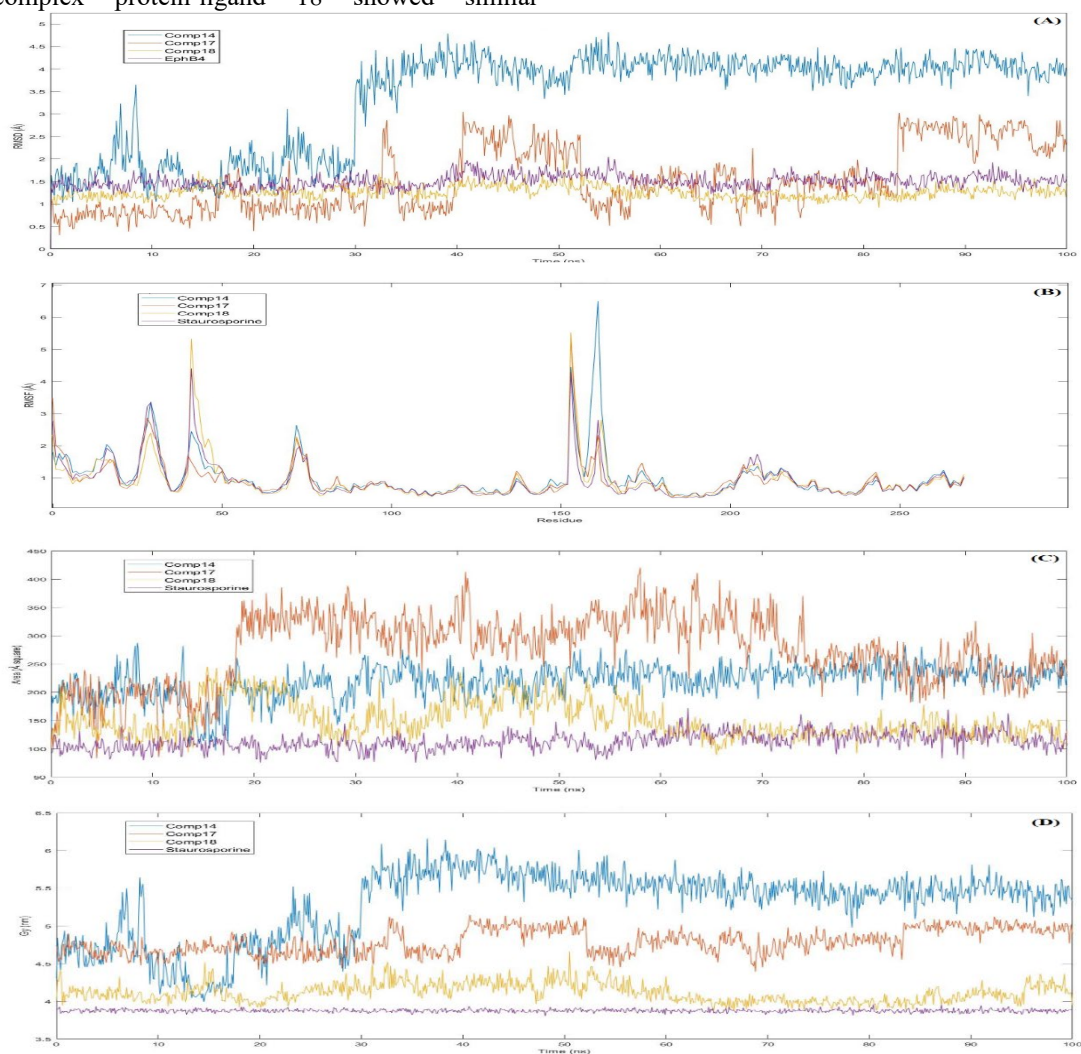


Figure 5. (A) RMSD (c-alpha), (B) RMSF, (C) Solvent accessible surface and (D) radius of gyration

The stability of the ligand in the protein binding pocket was further investigated by estimating and analysing the surface area of the ligands accessible by water molecules (Figure.5C). All systems' solvent accessible surface areas by ligands were found to be between 75 and 420Å², suggesting that the ligands were submerged in the binding pocket for the entire simulation period. The radius of gyration is a measure of the compactness of the ligand. Figure 5D illustrates that the radius of gyration values for all the systems were within the range of 3.80 and 6.16 nm. This suggests a stable ligand profile, which in turn supports the stable binding of the designed compounds and Staurosporine.

Stability of protein-ligand complexes has been proven by the MD simulation analysis of the docked complexes. Compound 18 was identified as a promising treatment candidate after 100 ns MD simulations of EphB4 and its suspected inhibitors. It had a high binding energy value, the best RMSD, RMSF, radius of gyration, and SASA parameters.

4. Conclusions

In recent times, fragment-based drug design has demonstrated its effectiveness as a method for drugs development. The ultimate objective of the current work is to discover novel EphB4 receptor tyrosine kinase inhibitors by using an in-silico drug design approach. For the study, an extensive number of different fragments with both natural and

Amine Ballari, Rachid Haloui, Ossama Daoui, Khaoula Mkhayar, Khadija Khaddam Allah, Samir Chtita, Abdelmoula El Abbouchi, Souad Elkhattabi

chemical sources were collected. The initial screening of the fragments was conducted using the rule of three. Applying molecular docking, the resultant fragments were screened against EphB4. To create 100 new compounds, fragment linking was applied to the highest-scoring fragments. Lipinski's rule of five, pharmacokinetic parameter prediction, and molecular docking against the EphB4 were used to define the 20 best compounds. Molecular dynamics was used to examine the ligand-protein complex stability of the three highest-scoring compounds and Staurosporine as a reference drug. The results were encouraging. The developed compounds were found to be more effective EphB4 receptor tyrosine kinase inhibitors in the current study when compared to the reference molecule. Thus, we were able to obtain possible EphB4 inhibitors by the use of in silico fragment-based drug design, which may be investigated further in the context of anti-cancer drug development.

Disclosure statement

No potential conflict of interest was reported by the authors.

Funding

No funding was received for this work.

References

- [1] L. R. de Souza Neto, J. T. Moreira-Filho, B. J. Neves, R. L. B. R. Maidana, A. C. R. Guimarães, N. Furnham, C. H. Andrade, F. P. Silva, In silico Strategies to Support Fragment-to-Lead Optimization in Drug Discovery. *Frontiers in chemistry* 8 (2020) 93.
- [2] M. K. Paul, A. K. Mukhopadhyay, Tyrosine kinase-Role and significance in Cancer, *International journal of medical sciences* 1 (2004) 101–115.
- [3] C. C. Ayala-Aguilera, T. Valero, Á. Lorente-Macías, D. J. Baillache, S. Croke, A. Unciti-Broceta, *Small Molecule Kinase Inhibitor Drugs (1995-2021): Medical Indication, Pharmacology, and Synthesis*, *Journal of medicinal chemistry* 65 (2022), 1047–1131.
- [4] J. Rudolph, J. J. Crawford, K. P. Hoeflich, J. Chernoff, p21-activated kinase inhibitors, *The Enzymes* 34 (2013) 157–180.
- [5] K. Kullander, R. Klein, Mechanisms and functions of Eph and ephrin signalling, *Nature reviews. Molecular cell biology* 3 (2002) 475–486.
- [6] R. Salgia, P. Kulkarni, P. S. Gill, EphB4: A promising target for upper aerodigestive malignancies, *Biochimica et biophysica acta. Reviews on cancer* 1869 (2018), 128–137.
- [7] Q. Li, Application of Fragment-Based Drug Discovery to Versatile Targets, *Frontiers in molecular biosciences* 7 (2020), 180.
- [8] J. Mortier, C. Rakers, R. Frederick, G. Wolber, Computational Tools for In Silico Fragment-Based Drug Design, *Current topics in medicinal chemistry* 12 (2012), 1935–1943.
- [9] Schrödinger Release 2024-3: Maestro, Schrödinger, LLC, New York, NY, 2024.
- [10] <https://www.rcsb.org/structure/3ZEW> December 2013, Accessed: 10.12.2023.
- [11] Schrödinger Release 2024-3: Protein Preparation Wizard; Epik, Schrödinger, LLC, New York, NY, 2024; Impact, Schrödinger, LLC, New York, NY; Prime, Schrödinger, LLC, New York, NY, 2024.
- [12] Schrödinger Release 2020-3: LigPrep, Schrödinger, LLC, New York, NY, 2020.
- [13] Schrödinger Release 2020-3: Glide, Schrödinger, LLC, New York, NY, (2020).
- [14] C. Choudhury, Fragment tailoring strategy to design novel chemical entities as potential binders of novel corona virus main protease, *Journal of biomolecular structure & dynamics* 39 (2021) 3733–3746.
- [15] Schrödinger Release 2024-3: QikProp, Schrödinger, LLC, New York, NY, 2024.
- [16] T. Darden, D. York, L. Pedersen, Particle mesh Ewald: An Mlog(N) method for Ewald sums in large systems, *Journal of Chemical Physics* 98 (1993) 10089–10092.
- [17] H. Jhoti, G. Williams, D. C. Rees, C. W. Murray, The “rule of three” for fragment-based drug discovery: where are we now?, *Nature Reviews Drug Discovery* 12 (2013), 644.
- [18] S. Genheden, U. Ryde, The MM/PBSA and MM/GBSA methods to estimate ligand-

Amine Ballari, Rachid Haloui, Ossama Daoui, Khaoula Mkhayar, Khadija Khaddam Allah, Samir Chtita, Abdelmoula El Abbouchi, Souad Elkhattabi

binding affinities, Expert opinion on drug discovery, 10 (2015) 449–461.

- [19] C. A. Lipinski, F. Lombardo, B. W. Dominy, P. J. Feeney, Experimental and computational approaches to estimate solubility and permeability in drug discovery and development settings, *Advanced drug delivery reviews* 46 (2001) 3–26.
- [20] D. F. Veber, S. R. Johnson, H. Y. Cheng, B. R. Smith, K. W. Ward, and K. D. Kopple, Molecular properties that influence the oral bioavailability of drug candidates, *Journal of medicinal chemistry* 45 (2002) 2615–2623.